3-8-2013

Monolayer-Protected Nanoparticle Doped Xerogels as Functional Components of Amperometric Glucose Biosensors

Michael Hartley Freeman

Jackson R. Hall

Michael C. Leopold
University of Richmond, mleopold@richmond.edu

Recommended Citation

M.H. Freeman, J.R. Hall, and M.C. Leopold, "Monolayer-Protected Nanoparticle Doped Xerogels as Functional Components of Amperometric Glucose Biosensors," *Analytical Chemistry* 2013, *85*(8), 4057-4065.

For submission to Analytical Chemistry

Monolayer-Protected Nanoparticle Doped Xerogels as Functional Components of Amperometric Glucose Biosensors

Michael H. Freeman, Jackson R. Hall and Michael C. Leopold*

Department of Chemistry, Gottwald Center for the Sciences, University of Richmond
Richmond, VA 23173

Abstract

First-generation amperometric glucose biosensors incorporating alkanethiolate-protected gold nanoparticles, monolayer protected clusters (MPCs), within a xerogel matrix are investigated as model systems for nanomaterial-assisted electrochemical sensing strategies. The xerogel biosensors are comprised of platinum electrodes modified with composite films of (3-mercaptopropyl)trimethoxy silane xerogel embedded with glucose oxidase enzyme, doped with $Au_{225}(C6)_{75}$ MPCs, and coated with an outer polyurethane layer. Electrochemistry and scanning/transmission electron microscopy, including cross-sectional TEM, show sensor construction, humidity effects on xerogel structure, and successful incorporation of MPCs. Analytical performance of the biosensor scheme with and without MPC doping of the xerogel is determined from direct glucose injection during amperometry. MPC-doped xerogels yield significant enhancement of several sensor attributes compared to analogous films without nanoparticles: doubling of the linear range, sensitivity enhancement by an order of magnitude, and four-fold faster response times accompany long term stability and resistance to common interferents that are competitive with current glucose biosensing literature. Ligand chain length and MPC:silane ratio studies suggest the MPC-induced enhancements are critically related to structure-function relationships, particularly those affecting inter-particle electronic communication where the MPC network behaves as a three-dimensional extension of the working electrode into the xerogel film, reducing the system's dependence on diffusion and maximizing efficiency of the sensing mechanism. The integration of MPCs as a functional component of amperometric biosensor schemes has implications for future development of biosensors targeting clinically relevant species.

---

* To whom correspondence should be addressed. Email: mleopold@richmond.edu. Phone: (804) 287-6329. Fax: (804) 287-1897

■ INTRODUCTION

Biosensor development has been of great interest in recent years due to expanding clinical and industrial applications.[1-3] Enzyme-based, electrochemical biosensors are a popular subdivision of this field as they are capable of providing a high degree of sensitivity, selectivity, and reproducibility as well as rapid response times in the detection of small molecules. Specifically, "1st generation" amperometric biosenors employ immobilized oxidase enzyme which, when reacted with a specific analyte, produce hydrogen peroxide (H_2O_2) that is subsequently oxidized at a working electrode to yield a current response proportional to analyte concentration.[1] Sensors of this type have the advantage of simplicity and affordability while also allowing for relatively easy modification to a variety of different target species and potential miniaturization for *in vitro* and *in vivo* clinical applications.[4-5]

Glucose is an affordable and well-studied biosensor analyte with direct clinical applications in the treatment of diabetes via continuous glucose monitoring. Glucose biosensors make up roughly 85% of the total biosensor market with a significant amount of that effort exploring 1st-generation schemes that utilize glucose oxidase enzyme (GOx) to catalyze the oxidation of glucose and generate electrochemically detectable H_2O_2 as an indirect determination of glucose. The significant amount of literature dedicated to glucose biosensing, as well as the availability of the materials, allow for the glucose/GOx system to serve as a model for exploring other aspects of 1st generation biosensing schemes, including signal enhancement and sensor performance tactics that may extend the strategy to additional species with physiological and clinical relevance.[6-7]

One of the challenges in developing functional amperometric enzymatic biosensors is the immobilization of enzymes at the electrode in high enough quantity to achieve sufficient signal-to-noise (S/N) without compromising the structural integrity and/or functionality of the enzymes. Many techniques have been employed to immobilize enzymes for biosensing purposes, including electropolymerization,[8] nanoporous gold,[9] hydrogels,[10] and sol-gels,[11] for example. Sol-gel networks are an attractive scaffold for multi-layer enzyme immobilization at an electrode because the silicate network is able to be formed under very mild conditions and exhibits inertness, rigidity, and negligible swelling in aqueous solution while still preserving the native structure/function of the encapsulated enzymes.[12-13] Moreover, the structural features of a sol-gel material, including porosity, hydrophobicity, biocompatibility, and mechanical stability, are easily manipulated based on the silane precursor(s) structures, silane-to-water ratio, addition of acid/base catalysts or solvents, and conditions during the gel's aging process.[14-15] Experimental controls of the film properties largely stem from fine-tuning of the hydrolysis and condensation sol-gel reactions. The resulting three-dimensional matrix of the xerogel is able to assist in selective permeability/diffusion of components of the enzymatic reaction, including the

target substrate (e.g. glucose), oxygen co-factor, as well as the H_2O_2 by-product that indirectly signals the presence of analyte.

Incorporation of certain nanomaterials (NMs), such as metallic nanoparticles (NPs) and nanotubes (NTs), into sol-gel matrices has become a prominent aspect of recent biosensing strategies. The unique characteristics of these materials, particularly with regard to their electron transfer (ET) properties, have encouraged their exploration as a functional component of biosensing schemes. Several reviews outline research activity on incorporating NMs into enzyme-doped sol-gel matrices.[16-17] Metallic NPs, particularly those of gold, have received considerable interest as their various synthetic routes provide customization of size, shape, and peripheral functionality with regard to the colloidal stabilizing ligands. Literature reports by Niemeyer[18] and Rotello[19] highlight the advantages of interfacing colloidal gold NPs with biomolecules, including large surface-to-volume ratios for adsorbate contact, adsorption microenvironment control for structural/orientation considerations, as well as the propensity of the NP network to act as a conduit, facilitating ET reactions. Since 2008, research aimed exclusively at incorporating NPs into electrochemical glucose sensors is nicely summarized in recent reviews.[20-21] In most cases, the justification for incorporating NPs in biosensing schemes is to elicit some sort of enhanced electrochemical signal.

A narrower body of work, including several reviews, focuses specifically on the use of colloidal gold NPs, commonly citrate stabilized gold NPs (CS-NPs), as a functional component of thin film or sol-gel based 1st generation glucose biosensors.[22-28] Most of these reports for amperometric glucose detection via NP/sol-gel composites are significantly limited in scope, focusing almost exclusively on proof-of-concept sensor performance rather than fundamental delineation of the exact role of the embedded NPs in order to broaden the applicability of the overall approach. The performance of the NP/sol-gel sensors described in these studies is of mixed success, sometimes suffering from insufficient linear ranges for physiological glucose concentrations,[24,26] slow response times,[27] poorly resolved amperometric responses,[24,26] or unaddressed issues of variability and/or stability.[20] Given the significant gaps in our fundamental knowledge regarding these systems, a thorough investigation of NP-embedded biosensors aimed at achieving a greater understanding of the structure-function relationships affecting sensing performance remains a study of significant value to the field.

Amperometric glucose biosensing systems involving sol-gels with NPs utilize silane precursors such as (3-methyl)trimethoxy silane (3-MTMOS) or similar molecules (e.g., TMOS, TEOS, or APTEOS) with systems embedding gold NPs such as CS-NPs employing (3-mercaptopropyl)trimethoxy silane (3-MPTMS) to allow for thiol-gold covalent interactions. In spite of their literature prominence[29] alkanethiolate-protected NPs, or monolayer-protected clusters (MPCs), remain a notable absence from the aforementioned body of work on NP-embedded sol-gel-based biosensors. Given some of the inherent

properties of MPCs, including high stability, ease of functionalization,[30] and a well-studied ability to promote extremely fast electron hopping,[29] their omission in this capacity is that much more curious.

Our research over the past several years has focused on MPC networks as an interface for protein immobilization and subsequent biological ET reactions in the form of protein monolayer electrochemistry (PME).[31] Three principal findings suggest that the incorporation of MPC-doped sol-gels may have significant merit for biosensing schemes: (1) PME schemes employing electrode platforms such as self-assembled monolayers (SAMs) or NP film assemblies are restricted to a monolayer or less of active biomolecules and have limited S/N capacity;[31] (2) MPC networks provide homogeneous adsorption environment for proteins while maintaining their structure/function;[32] and (3) MPC networks promote very fast ET through the film over significant distances through synthetic films.[33] All three of these findings encourage the hypothesis that MPC networks embedded within a sol-gel may serve as an effective scaffold for multi-layers of enzymes, allowing for more efficient 1st generation biosensing with substantially greater S/N.

In this work, we examine the incorporation of MPCs as a functional component of enzyme-embedded sol-gel within a 1st generation amperometric biosensor scheme. To our knowledge, this is the first study of its kind to substantially explore the highly stable and versatile MPCs in an amperometric biosensing capacity of this nature. Using glucose/GOx as a model system, we present biosensors with GOx embedded 3-MPTMS xerogels doped with MPCs and coated with an outer, semi-permeable, blended polyurethane (PU) layer, a common outer membrane used in amperometric biosensing schemes.[34-35] Our research includes extensive characterization of the biosensor assembly with specific incorporation of the NPs as well as traditional quantitative analysis of the sensor's performance parameters. Beyond the proof-of-concept demonstration of MPC networks being a viable and effective biosensing component that enhances sensor performance, this research also probes critical MPC structure-function relationships that impact sensor function and identifies key sources of variability. On a broader spectrum, the demonstrated use of MPC-doped xerogels as part of biosensing schemes provide insight to a general approach of utilizing the versatility of MPCs to specifically tailor systems for a range of specific physiological targets with clinical relevance (e.g., lactate,[34,36] cholesterol,[37] uric acid,[38] for examples).

■ EXPERIMENTAL SECTION

Materials and Instrumentation

All chemicals were purchased from Sigma Aldrich unless otherwise stated. Tecoflex SG-80A polyurethane (TPU) and Hydrothane AL25-80A polyurethane (HPU) were obtained from Lubrizol and AdvanSource Biomaterials, respectively. All solutions were prepared using 18.2 MΩ ultra-purified (UP)

water. The analytical performance of the sensors was evaluated via amperometric current-time (*I-t*) curves recorded with an eight channel potentiostat (CH Instruments, 1000B) with electrochemical cells composed of modified 2 mm diameter Pt working electrodes, a common Ag/AgCl (satr'd KCl) reference electrode (CH Instruments), and a common platinum wire counter electrode.

Alkanethiolate-protected MPCs with an average structure of $Au_{225}(C6)_{75}$ and core diameter (d) of 2.0 (± 0.8) nm were synthesized via minor modifications to the well-known Brust reaction[39] with the product characterized as prepared or after place-exchange modification[30] as in previous reports using NMR and TEM. Details of the synthesis and characterization procedures are included as part of the Supporting Information with the results found consistent with prior work.[29,31,33,40]

Preparation of MPC-doped amperometric sol-gel biosensors

Platinum disk working electrodes were polished successively with 1, 0.3, and 0.05 μm alumina powder and UP H_2O on a polishing wheel. Polished electrodes were subjected to cyclic voltammetry in 0.1M H_2SO_4 between potentials of +1.2 V and -0.25 V at 0.25 V/s until voltammogram was consistent with that of a clean platinum surface.

To fabricate the xerogel layer, 3-MPTMS, stored in a dessicated glove box (Plas Labs, Inc.) and renewed every 2-3 weeks, was transferred under dry environment to 2 mL centrifugation vials which were then capped and sealed within a smaller, portable dessicator. **Notice:** *Strict relatively humidity (RH) control, through the use of dessicated glove boxes/vessels during storage/handling of silanes as well as with a humidity-controlled chamber (Cole-Parmer) during deposition/drying of the sol-gels was found to be critical for consistent sensor performance*. Control sol-gel mixtures (i.e., without MPC doping) were prepared as described in literature reports[35] by first dissolving 9.0 mg of glucose oxidase (GOx) in 75 μL of UP H_2O in a centrifugation vial and, in a separate vial, diluting 25 μL of 3-MPTMS with 100 μL of THF. These vials were sealed and vigorously shaken inside the controlled-humidity chamber (50% RH). After 10 minutes of individual mixing, 50 μL of the GOx/H_2O solution was transferred under controlled humidity to the vial containing the 3-MPTMS/THF mixture and shaken for an additional 10 minutes to facilitate the formation of a sol-gel. A 3 μL aliquot of the sol-gel mixture was then directly deposited onto the platinum electrodes inside the humidity chamber. Unless otherwise stated, sol-gel coated electrodes were allowed to form xerogels over 48 hours inside the chamber (50% RH). Sol-gel structure was assessed using SEM imaging and MPC incorporation into the xerogels was verified using TEM, including a previously established cross-sectional TEM procedure used to assess film thickness (Supporting Information). For MPC-doped xerogels, the aforementioned procedure typically included adding 19.0 mg of MPCs to the initial 3-MPTMS/THF solution (1:400 ratio of MPC-to-silane).

The polyurethane (PU) mixture was prepared as reported in the literature,[35] where a specific blend of polymers, previously shown as an effective permiselective membrane, allow glucose and oxygen diffusion while reducing penetration of common interferents.[35] PU is prepared by adding 50 mg of TPU and HPU to a 5 mL solution of THF/EtOH (50:50 v/v) and sonicating until the materials completely dissolve. A 10 μL aliquot of blended PU mixture was deposited atop the dried (48 hr.) enzyme-bedded xerogel and allowed to dry completely (30 min.).[35]

Evaluation of glucose biosensor performance

Completed sensors were soaked in 4.4 mM potassium phosphate buffer solution (PBS) at pH 7 for a minimum of 1 hour to reduce current drift and impregnate the sol-gel with solution. All biosensors were subjected to +0.65V in 25 mL PBS for 20 minutes prior to injection of any glucose to stabilize sensor reading. Aliquots of 1M glucose stock solution were injected at 100 second intervals while stirring to obtain steady state sensor response to successive 1 mM glucose increases. For longer term stability tests, sensors were stored soaked in PBS at 7ºC and tested periodically over 45 days.

■ RESULTS AND DISCUSSION

Assembly and Characterization of MPC-Doped Sol-Gel Biosensors

Our 1st generation biosensor design (**Figure 1**) features an enzyme encapsulating xerogel layer doped with nanoparticles (NPs) and covered with an interfacial, multi-functional adlayer of polyurethane (PU). As described in the Experimental Section, the biosensor is constructed at a platinum working electrode using a "sandwiching" or layering technique previously shown to be effective by our group and others.[12,35,41] The xerogel is formed through traditional sol-gel chemistry using 3-MPTMS, a common silane in sol-gel literature reporting stable encapsulation of enzymes and thiol-centered anchoring of gold-based NPs within gel's network.[36,42] To our knowledge, however, the incorporation of alkanethiolate-protected gold nanoparticles or MPCs into a biosensing scheme of this nature is unprecedented. Specifically, the sol-gel is doped with hexanethiolate-stabilized gold nanoparticles ($Au_{225}(C6)_{75}$), hereafter referred to as C6 MPCs, which have well-established stability and versatility compared to other colloidal metal NPs (e.g., CS-NPs[41]). Since the focus of our study is the role and benefit of NP networks within the 1st generation biosensing scheme, we have employed glucose/glucose oxidase (GOx) as a simple, model system. The specific PU layer used, a 50:50 (w/w) blend of hydrophilic and hydrophobic polyethers as well as the deposition volume (thickness), has been well-established in the literature for electrochemical glucose sensors,[35] and serves several functions, including preventing GOx leeching from the sol-gel, promoting O_2 and glucose diffusion, confining the H_2O_2 by-product at the platinum electrode, and providing additional selectivity via impermeability to several common interferents.[22,35,43-44]

In constructing these biosensors, the sol-gels are formed with co-encapsulation of GOx (8 nm diameter) and C6 MPCs to form a porous composite structure illustrated pictorially in **Figure 1.** To confirm the incorporation of C6 MPCs into the sol-gels, materials with and without embedded nanoparticles were extensively characterized with different forms of microscopy and electrochemistry. **Figure 2** shows scanning electron microscopy (SEM) imaging of C6 MPC-doped xerogels (3-MPTMS) and reveals the highly porous surface structure with significant internal structure within individual pores. Imaging of analogous sol-gel material without MPCs shows substantially lower porosity (Supporting Information). As discussed further in a later section and Supporting Information, SEM also proved useful for showing the critical nature of humidity and/or drying time of the sol-gels. The most stable films, used herein, were found to be those deposited and stored at 50% RH before being used as sensors.

Transmission electron microscopy (TEM) imaging was used to confirm the presence of the metallic C6 MPCs within the sol-gel films as well as for an accurate measurement of the xerogel thickness being employed for the sensors. **Figure 3** shows TEM images of 3-MPTMS sol-gel films with and without MPC doping. A lack of contrast in TEM images of films without MPCs is expected whereas images of MPC-doped films clearly show the presence of the nanoparticles within the 3-MPTMS sol-gels, appearing as numerous dark masses with the expected size and shape of the MPCs ($d \sim 2.0 \pm 0.8$ nm).[30-33] Cross-sectional TEM imaging was used to assess the thickness of the xerogel layers typically incorporated into these biosensor schemes. We have successfully adapted a cross-sectional TEM imaging technique that was used for MPC film assemblies in prior work to generate the images like that shown in **Figure 3, inset**. Here, a cross section of a 3-MPTMS xerogel film is clearly discernible within the image and its thickness is easily measured. In a typical deposition procedure, the MPC-doped xerogel with embedded GOx is a film of approximate thickness of 2.0-2.5 μm as determined by this method. Additional TEM and cross-sectional TEM imaging of MPC-doped sol-gel films are included in Supporting Information. Taken collectively, microscopy characterization of the MPC-doped xerogel films suggest the structure is consistent with Figure 1B.

Electrochemical probing experiments and H_2O_2 permeability experiments were used to report the successful incorporation of C6 MPCs into the 3-MPTMS xerogel films. The voltammetry of freely diffusing ruthenium hexamine chloride, a common redox probe for modified electrodes,[14] was observed at a bare electrode and compared to sol-gel modification with and without embedded MPCs. Smaller voltammetry peak currents and increased peak splitting were observed when a 3-MPTMS sol-gel is used to modify the electrode, a result consistent with blocking behavior at modified electrodes. Upon impregnating the xerogel with a hydrophobic network of C6 MPCs, the ruthenium hexamine probe becomes completely blocked from the electrode and exhibits no voltammetric signal, a result suggesting the MPCs have been integrated into the material (Supporting Information).

As reported for layered film assemblies,[35] H_2O_2 permeability can be used to follow the effectiveness of the different components comprising the biosensor and also verify MPC incorporation into these particular sensors. Biosensors, with and without MPC doping and PU capping layers, were immersed in PBS and monitored at +0.65 V during exposure to 250 μM H_2O_2 injections. From the resulting amperometric current-time (*I-t*) curves, the permeability index can be calculated by comparing anodic current H_2O_2 oxidation at the bare platinum electrode to the current passed at electrodes modified with different components. Consistent with the electrochemical probing results, modification of the electrode with un-doped 3-MPTMS sol-gel results in a significant decrease in the H_2O_2 permeability index, measuring ~15% while modification with an analogous film with embedded MPCs results in an even smaller H_2O_2 permeability index (~8%). In both cases, with and without MPC doping, H_2O_2 permeability is halved when the PU capping layer is added (Supporting Information). The increased blocking of H_2O_2 from the solution interface is noteworthy as it shows the PU is an effective H_2O_2 barrier and will restrict enzymatically generated H_2O_2 to the platinum electrode for more efficient oxidation that is beneficial for sensing performance.

Analytical Performance of MPC-Doped Sol-Gel Biosensors

The analytical performance of the MPC-doped sol-gel biosensors, including dynamic/linear range of the amperometric step response, response time, response to interferents, and variability were compared to analogous systems without MPCs. According to Figure 1, sensors were constructed with and without MPC doping of the GOx/xerogel layer. C6 MPCs were incorporated into the sol-gel mixture in a 400:1 silane-to-MPC ratio as a standard procedure before being deposited on the electrode. After assembly and pretreatment (Experimental Section), the sensors were immersed in stirred PBS and their amperometry monitored during successive injections at 100 second intervals that resulted in incremental 1 mM glucose concentrations. Typical real-time, amperometric *I-t* curves for biosensors with and without MPC doping are shown in **Figure 4** and illustrate a notable difference in observed response observed between the two systems. The MPC-doped xerogels exhibit a significantly greater current response toward glucose compared to sensors without incorporated MPCs (Figure 4, left expansion). Furthermore, consistent, well-defined amperometric step responses are observed for nearly 30 consecutive glucose injections (28 mM glucose), at the MPC-doped system, a range that easily spans normal physiological levels of glucose (4-7 mM^{-1}). Alternately, systems without MPC co-encapsulated with GOx in the sol-gel display smaller and less-defined step response over a concentration range less than half that of the MPC-doped system before exhibiting no step response at all (Figure 4, right expansion).

Calibration curves for the glucose sensors with and without MPC doping are compiled in **Figure 5A**. It is readily apparent from the results that including MPCs as a component of the sensing scheme

results in several noteworthy advances in performance. The MPC systems possess a significantly higher (>2.5x) sensitivity ($0.072_{(\pm 0.002)}$ μA/mM vs. $0.184_{(\pm 0.005)}$ μA/mM), a more persistent step response (i.e., dynamic range) to higher concentrations of glucose ($12_{(\pm 1)}$ mM vs. $22_{(\pm 1)}$ mM), as well as a rather substantial increase (doubling) of the linear range for glucose detection. Whereas both systems exhibit large dynamic ranges, the significantly extended linear range achieved with MPC incorporation is highly reproducible and directly attributable to the MPC inclusion. The limit of detection ($3\sigma_{BL}$) for the MPC-doped xerogel glucose sensors was determined to be $23.2_{(\pm 5.5)}$ μM, well below even the lower limit of relevant physiological glucose concentrations. It is noteworthy that the sensitivity, linear/dynamic range, and limit of detection for MPC-doped xerogel sensors, as well as their response times and interferent discrimination (discussed below), all equal or exceed the performance of sol-gel-based glucose sensors with and without NP doping in the literature (Supporting Materials – Table SM-1).

Qualitative inspection of the two types of step responses for these systems (Figure 5) also suggests that the inclusion of the network of MPCs within the xerogel sensor results in faster response times for reporting solution glucose. That is, the step response with MPCs is an immediate and sharp step compared to a more gradual sloping step response for systems without MPCs. A more quantitative comparison of response times, as performed in similar biosensing papers,[35] is determined by taking the average current response 10 seconds prior to injection for two consecutive steps, calculating the total change in current, and determining the time it takes to reach 95% of that total response ($t_{r,95\%}$). **Figure 5B** shows the $t_{r,95\%}$ of MPC-doped xerogel glucose biosensors compared to those without MPCs. The addition of MPCs to the sol-gel structure appears to have substantial effect on $t_{r,95\%}$, decreasing it by a factor of 4 for the 1st step response, for example. The lower $t_{r,95\%}$ of the MPC-doped sensors continues at later steps as well, while the sensors without MPCs fail to give step responses after only about 10 injections of glucose (10 mM glucose). The observed enhancement of sensitivity and response time due to the incorporation of the MPC networks are quite stable and were monitored for over two weeks without significant change (**Figure 6**). We note there was slightly more variability for response time upon initial (i.e., Day 0) testing (not shown), suggesting that the pre-conditioning soak in PBS may be an important aspect of achieving stable performance. Response times during recorded over increasing glucose concentration ranges (i.e., 0-1 mM, 5-6 mM, and 10-11 mM injections) indicate that the enhanced sensing response achieved with the MPC doping of the xerogels persists well across the relevant physiological range of glucose for over two weeks as well. Long term testing of the sensor after 45 days showed only a modest degradation of sensitivity and response time (Supporting Information).

To assess interferent response, amperometric selectivity coefficients (K^{amp}) for specific interferents were calculated by comparing ratios of measured currents-to-concentration for a specific interferent and a standard glucose response (1mM) (Supporting Information).[5,35,45] The 3-MPTMS sol-gel-based biosensors

in this study were tested versus an array of the most common, endogenous physiological interferents for glucose sensing including ascorbic acid, sodium nitrite, uric acid and oxalic acid.[22,35,43] Additionally, acetaminophen, a known synthetic glucose analogue identified as one of the most difficult interferent species to discriminate against[22] was also tested.[35] Amperometry during the injection of the different interferent species (100 μM) compared to glucose (1 mM) at PU-coated xerogel sensors with and without C6-MPC doping resulted in *I-t* responses that were translated to K_{amp} values (Supporting Information). The K_{amp} for most of the interferents are consistent with other reports using this parameter and are considered adequate for the selective detection of glucose.[5,35,45] For example, studying PU-capped, MTMOS/xerogel glucose sensors doped with silica NPs, Koh and coworkers reported individual K_{amp} values for ascorbic acid (0.55), sodium nitrite (-0.17), and uric acid (0.88).[35] Selectivity coefficients for these same three species at C6 MPC-doped xerogels with a PU outer layer were 0.39, 0.04, and no response, respectively. Consistent with our results, Rodriguez-Amaro reported no response toward oxalic and uric acid and an estimated selectivity coefficient for ascorbic acid of 0.65.[22]

A major finding of our work on these biosensors is their susceptibility to performance variability. The sensors required extensive and meticulous controls during experiments as well as with the storage of materials in order to achieve adequate reproducibility. As alluded to in the characterization section, the most important factors identified for performance and reproducibility of these sensors were RH during film formation and drying. Calibration curves from xerogel sensors with and without MPC doping that were allowed to dry at varying times (2, 24 and 48 hours) indicate that increased drying time, in addition to MPC incorporation, significantly increase sensitivity and were used to establish the standard protocol of 48 hour drying under 50% RH as optimal. Data collected without controls on both humidity and drying time showed significant variability (Supporting Information). When MPC-doped films were allowed to dry for less than 48 hours, resulting in a significantly lower current response, two key MPC-related observations still persisted, a significantly extended linear range as well as faster response time (Supporting Information).

Another factor identified that had a significant impact on film-to-film variability of sensor response was the composition of the sol-gel during deposition. Our results suggest that the deposition solution requires intensive and consistent mixing prior to the application to the electrode with the deposition aliquot withdrawn from the bottom of the mixing vessel. Failure to comply with these standards of mixing/sampling had a significant impact on the step-response, including if the higher or lower current response/sensitivity was observed. The deposition mixture is complex, with two different solvents (water and THF) of different densities/solubility toward MPC and 3-MPTMS. Consistent with sol-gel literature,[46] the water-to-silane ratio in the deposition aliquot from the mixture will likely affect the porosity of the sol-gel formed at the electrode (Supporting Information). Other sources of variability

including GOx and 3-MPTMS age, different MPC batches, and THF dryness were determined to be of less significant than humidity, dry time, and deposition composition (results not shown).

Response Mechanism of MPC-Doped Sol-Gel Biosensors

One of the more differentiating aspects of this study was experimentation designed to better understand and specifically define the functional contribution of the MPC network within the biosensing mechanism. Experiments were designed to see if the enhancements achieved with incorporating MPCs could be "turned off" with strategic manipulations of the MPC network. Hypothesizing that part of the signal enhancement mechanism was related to the intra-film electronic coupling between the MPCs within the xerogel, sensors were designed varying the ratio of MPC-to-silane in the sol-gel deposition mixtures as a means of diluting inter-particle coupling and assessing its effect on performance. Results from sol-gel mixtures contained different MPC:silane ratios (1:400 vs. 1:1600) were compared to mixtures with no MPC doping (**Figure 7**). From these results, one can infer that dilution of C6 MPCs prior to drop casting has a significant effect on sensor performance, significantly lowering the observed sensitivity in the calibration curve comparison, though still outperforming films without any MPC doping.

A second type of experiment conducted to delineate specific structure-function relationships in MPC-modified biosensor schemes and further probe the importance of inter-particle electronic coupling was the alteration of the peripheral ligands of the MPCs. One of the advantages encapsulating alkanethiolate-based NPs such as MPCs is that their ligands, and subsequently their surface chemistry (e.g., functionality, hydrophobicity, chain length) can be readily manipulated with simple place-exchange reactions.[30-31] Dodecanethiolate-protected (C12) MPCs were synthesized and doped into 3-MPTMS xerogels in the same manner and amount as the C6 MPCs. **Figure 8** illustrates the typical, real-time *I-t* response and calibration curves comparing xerogel glucose sensors doped with C6 or C12 MPCs. As seen in the results, C6 MPC-doped sensors perform as previously described, yielding well-defined step responses and fast response times (Fig. 8A, inset) to glucose injections up to 20 mM, with a linear and dynamic range up to 12 and 28 mM, respectively. The C12 MPC films, however, perform with strikingly less sensitivity and approximately half the range of step (≤ 12 mM) and linear (≤ 8 mM) responses to glucose.

If the MPC network is behaving as a three-dimensional extension of the working electrode within the xerogel, the reduction in sensitivity and corresponding increase in response time may be explained in two ways. First, the longer and more hydrophobic C12 MPCs may simply be more efficient at blocking H_2O_2 diffusion to the MPC nanoelectrodes. The decreased response of common interferents (e.g., acetaminophen, ascorbic acid) at C12 MPC-doped sol-gel films bolsters this scenario. Interestingly, if the xerogel films are doped with C6 MPCs that have undergone place-exchange reactions with 11-

mercaptoundecanoic acid (MUA), or C6/MUA MPCs, the K^{app} values of these two interferents are increased to levels at or above that observed for C6 MPCs (Supporting Information). These preliminary C6/MUA MPC doping results imply that hydrophobicity may be a significant factor affecting analyte/interferent diffusion. If H_2O_2 oxidation does occur at the MPC gold cores within the sol-gel, however, the resulting signal enhancement is likely related to the very fast electronic communication through the MPC network to the electrode, a phenomenon known as "electron hopping."[29,31,33] In that case, the C12 periphery of the MPCs in the films may effectively decouple the NPs from each other, severely hampering the inner film ET communication.[47] Further study will be required to elucidate which one of these two effects is more dominant. While the mechanism is not yet fully resolved, collectively, these two results (Figures 7 and 8) suggest that the MPCs are playing a critical role in enhancing the signal but that their contribution can be severely diminished by either diluting the amount of MPC within the film or by significantly increasing the thickness of the organic periphery of the MPCs – both of which are believed to induce electronic decoupling within the MPC network.

■ CONCLUSIONS

The incorporation of NPs into sol-gel-based electrochemical biosensors remains an interesting strategy for sensor technology development. Previously unexplored, the doping of thiolate-protected NPs or MPCs doped into 3-MPTMS xerogels for 1st generation amperometric glucose biosensing establishes a model system with significant attributes that include dramatic improvement of sensitivity, response times and linear range while still maintaining adequate interferent discrimination. Additionally, the MPCs offer unmatched NP stability and the potential for strategic functionalization through place-exchange reactions, a property unique to MPCs that may directly affect xerogel characterisitcs like hydrophobicity and porosity. The MPC-doped sol-gel glucose biosensors of this study equal or exceed comparable glucose biosensors reported in the literature, including those that utilize other types of NMs (Supporting Information). While the mechanism is not fully understood, the improved sensor performance is currently being attributed to an overall increase in the efficiency of the enzymatic and electrochemical reactions responsible for reporting the presence of solution glucose. Specifically, our results suggest that the MPC network within the sol-gel acts as a 3-dimensional extension of the working electrode area that allows for the biosensor's signal to have a decreased dependence on the diffusion of H_2O_2. Even at significant distance from the working electrode, H_2O_2 oxidation throughout the film is readily reported via fast ET through a highly stable electronic conduit – the MPC network. Future work with this model system will involve further elucidation of structure-function relationships (e.g., core size/polydispersity, ligand functionality, hydrophobicity) that affect sensor performance or allow greater understanding of the

MPCs' role in both the xerogel structure and the electrochemical reaction. The significance of these findings is the fundamental foundation for a general strategy of incorporating MPCs as functional components of biosensors as their versatility suggests similar biosensing schemes can be specifically designed from this template for the continuous, real-time *in vivo* or *in vitro* monitoring of clinically important compounds.[48-50]

■ ACKNOWLEDGEMENTS

We gratefully acknowledge the National Science Foundation (CHE-0847145), Howard Hughes Medical Institute (MHF and JRH), Henry Dreyfus Teacher-Scholar Award, and Chemistry Puryear-Topham (MHF) and Undergraduate Research Committee (JRH) funding from the University of Richmond for generously supporting this research. We specifically recognize Christie Davis (Department of Biology, Director of Microscopy) and Tran Doan for their assistance with TEM/SEM imaging and Dr. B.J. Privett and Ahyeon Koh (Schoenfisch Lab, UNC-CH) for helpful discussions.

■ REFERENCES

(1) Wang, J. *Chem. Rev.* **2008**, *108*, 814-825.
(2) Pohanka, M.; Skládal, P. *J. Applied Biomed.* **2008**, *6*, 57-64.

(3) Kerman, K.; Saito, M.; Tamiya, E.; Yamamura, S.; Takamura, Y. *TrAC, Trends Anal. Chem.* **2008**, *27*, 585-592.
(4) Wang, J. *Talanta.* **2008**, *75*, 636-641.
(5) Wilson, G. S.; Gifford, R. *Biosens. Bioelectron.* **2005**, *20*, 2388-2403.
(6) Parra, A.; Casero, E.; Vázquez, L.; Pariente, F.; Lorenzo, E. *Anal. Chim. Acta* **2006**, *555*, 308-315.
(7) Sanford, A. L.; Morton, S. W.; Whitehouse, K. L.; Oara, H. M.; Lugo-Morales, L. Z.; Roberts, J. G.; Sombers, L. A. *Anal. Chem.* **2010**, *82*, 5205-5210.
(8) Ciobanu, M.; Taylor, D. E., Jr.; Wilburn, J. P.; Cliffel, D. E. *Anal. Chem.* **2008**, *80*, 2717-2727.
(9) Gamero, M.; Pariente, F.; Lorenzo, E.; Alonso, C. *Biosens. Bioelectron.* **2010**, *25*, 2038-2044.
(10) Romero, M. R.; Garay, F.; Baruzzi, A. M. *Sens. Actuators, B.* **2008**, *B131*, 590-595.
(11) Walcarius, A.; Collinson, M. M. *Annu. Rev. Anal. Chem.* **2009**, *2*, 121-143.
(12) Narang, U.; Prasad, P. N.; Bright, F. V.; Ramanathan, K.; Kumar, N. D.; Malhotra, B. D.; Kamalasanan, M. N.; Chandra, S. *Anal. Chem.* **1994**, *66*, 3139-3144.
(13) Liu, S.; Sun, Y. *Biosens. Bioelectron.* **2007**, *22*, 905-911.
(14) Collinson, M. M.; Wang, H.; Makote, R.; Khramov, A. *J. Electroanal. Chem.* **2002**, *519*, 65-71.
(15) Sinko, K. *Materials.* **2010**, *3*, 704-740.
(16) Guo, S.; Dong, S. *TrAC Trends Anal. Chem.* **2009**, *28*, 96-109.
(17) Pandey, P.; Datta, M.; Malhotra, B. D. *Anal. Lett.* **2008**, *41*, 159-209.
(18) Niemeyer, M. *Angew Chem Int Ed Engl.* **2001**, *40*, 4128-4158.
(19) Shenhar, R.; Rotello, V. M. *Acc. Chem. Res.* **2003**, *36*, 549-561.
(20) Siangproh, W.; Dungchai, W.; Rattanarat, P.; Chailapakul, O. *Anal. Chim. Acta.* **2011**, *690*, 10-25.
(21) Wang, F. *Mikrochim. Acta* **2009**, *165*, 1-22.
(22) Sánchez-Obrero, G.; Cano, M.; Ávila, J. L.; Mayén, M.; Mena, M. L.; Pingarrón, J. M.; Rodríguez-Amaro, R. *J. Electroanal. Chem.* **2009**, *634*, 59-63.
(23) Feng, D.; Wang, F.; Chen, Z. *Sens. Actuators, B* **2009**, *138*, 539-544.
(24) Zhang, J. *Science in China.Series B, Chemistry.* **2009**, *52*, 815-820.
(25) Barbadillo, M.; Casero, E.; Petit-Domínguez, M. D.; Vázquez, L.; Pariente, F.; Lorenzo, E. *Talanta.* **2009**, *80*, 797-802.
(26) Zhang, S.; Wang, N.; Niu, Y.; Sun, C. *Sens. Actuators, B* **2005**, *109*, 367-374.
(27) Tang, F. *Science in China.Series B, Chemistry.* **2000**, *43*, 268-274.
(28) Pingarrón, J. M.; Yáñez-Sedeño, P.; González-Cortés, A. *Electrochim. Acta* **2008**, *53*, 5848-5866.
(29) Sardar, R.; Funston, A. M.; Mulvaney, P.; Murray, R. W. *Langmuir* **2009**, *25*, 13840-13851.
(30) Hostetler, M. J.; Templeton, A. C.; Murray, R. W. *Langmuir* **1999**, *15*, 3782-3789.
(31) Loftus, A. F.; Reighard, K. P.; Kapourales, S. A.; Leopold, M. C. *J. Am. Chem. Soc.* **2008**, *130*, 1649-1661.
(32) Doan, T. T.; Vargo, M. L.; Gerig, J. K.; Gulka, C. P.; Trawick, M. L.; Dattelbaum, J. D.; Leopold, M. C. *J. Colloid Interface Sci.* **2010**, *352*, 50-58.
(33) Vargo, M. L.; Gulka, C. P.; Gerig, J. K.; Manieri, C. M.; Dattelbaum, J. D.; Marks, C. B.; Lawrence, N. T.; Trawick, M. L.; Leopold, M. C. *Langmuir* **2010**, *26*, 560-569.
(34) Romero, M. R.; Ahumada, F.; Garay, F.; Baruzzi, A. M. *Anal. Chem.* **2010**, *82*, 5568-5572.
(35) Koh, A.; Riccio, D. A.; Sun, B.; Carpenter, A. W.; Nichols, S. P.; Schoenfisch, M. H. *Biosens. Bioelectron.* **2011**, *28*, 17-24.
(36) Parra-Alfambra, A. M.; Casero, E.; Petit-Dominguez, M. D.; Barbadillo, M.; Pariente, F.; Vazquez, L.; Lorenzo, E. *Analyst (Cambridge, U. K.).* **2011**, *136*, 340-347.
(37) Jiang, D.; Fang, D.; Kelley, T. J.; Burgess, J. D. *Anal. Chem.* **2008**, *80*, 1235-1239.
(38) Rawal, R.; Chawla, S.; Chauhan, N.; Dahiya, T.; Pundir, C. S. *Int. J. Biol. Macromolecules* **2012**, *50*, 112-118.
(39) Brust, M.; Fink, J.; Bethell, D.; Schiffrin, D. J.; Kiely, C. *J. Chem. Soc., Chem. Commun.J* **1995**, 1655-1656.
(40) Doan, T.; Freeman, M.; Schmidt, A.; Nguyen, N.; Leopold, M. *J. Visualized Exp.* **2011**, *56*,

e3441, [DOI: 10.3791/3441].
(41) Russell, L. E.; Galyean, A. A.; Notte, S. M.; Leopold, M. C. *Langmuir* **2007**, *23*, 7466.
(42) Jena, B. K.; Raj, C. R. *Electroanalysis* **2007**, *19*, 816-822.
(43) Yang, Y.; Tseng, T.; Lou, S. *IEEE*. **2007**, 6624-6627.
(44) Ward, W. K.; Jansen, L. B.; Anderson, E.; Reach, G.; Klein, J.; Wilson, G. S. *Biosens. Bioelectron*. **2002**, *17*, 181-189.
(45) Heller, A.; Feldman, B. *Chem. Rev*. **2008**, *108*, 2482-2505.
(46) Wright, J. D. and Sommerdijk, N. A. J. M. *Sol-Gel Materials Chemistry and Applications,* CRC Press:New York; 2001.
(47) Doan, T.; Day, R.; Leopold, M. *J. Mater. Sci*. **2011**, *47*, 108-120.
(48) Rong, Z. *IEEE* **2008**, *8*, 113-120.
(49) Qiang, L.; Vaddiraju, S.; Patel, D.; Papadimitrakopoulos, F. *Biosens. Bioelectron*. **2011**, *26*, 3755-3760.
(50) Yan, Q.; Major, T. C.; Bartlett, R. H.; Meyerhoff, M. E. *Biosens. Bioelectron*. **2011**, *26*, 4276-4282.

Figures and Schemes: Note: Sized to 8.25 cm (3.25") width (single column)

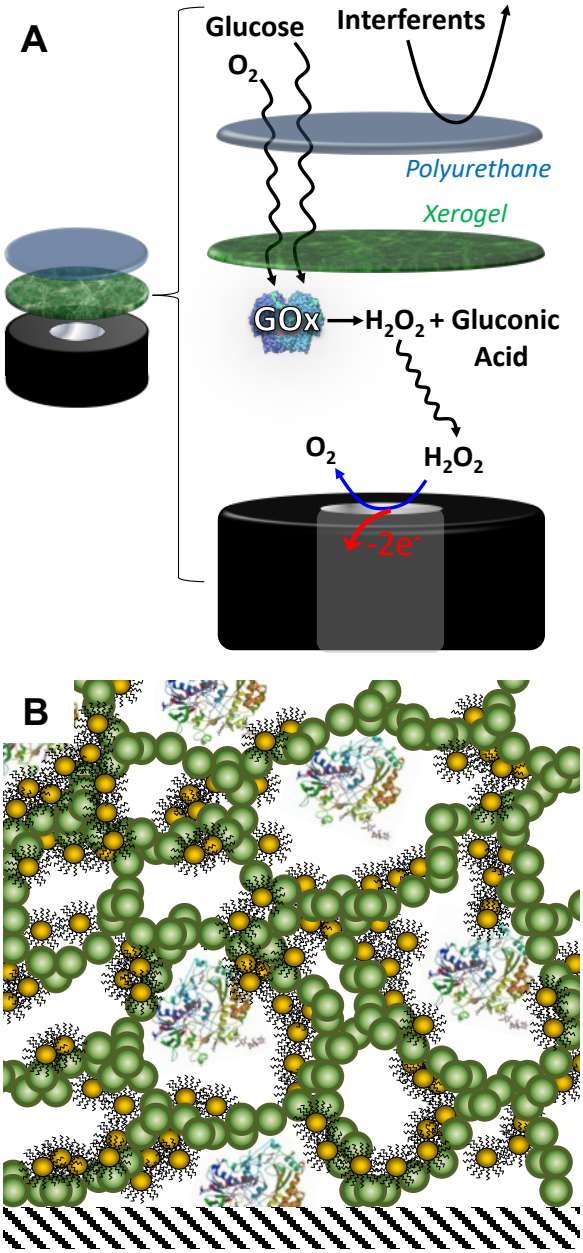

Figure 1. **(A)** Schematic illustration of 1st generation glucose biosensor scheme with GOx embedded in a MPTMS xerogel and capped with polyurethane; **(B)** Xerogel structure embedded with GOx and doped with C6-MPCs with average diameters of 8 and 2.0 (±0.8) nm, respectively.

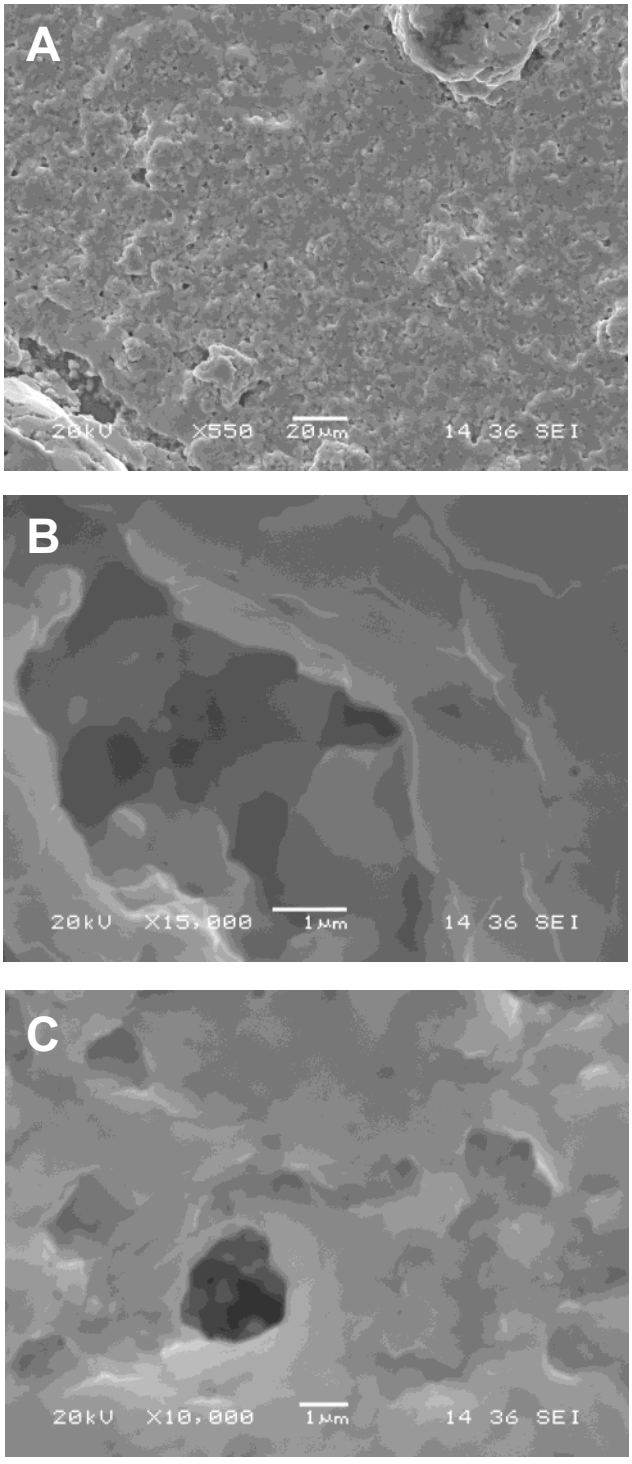

Figure 2. SEM imaging of MPC-doped MPTMS xerogels with embedded glucose oxidase (GOx) showing overall surface porosity (**A**) and magnified inner structure of pores (**B,C**). The size bars (*bottom, center*) in each image are 20 µm, 1 µm, and 1 µm, respectively.

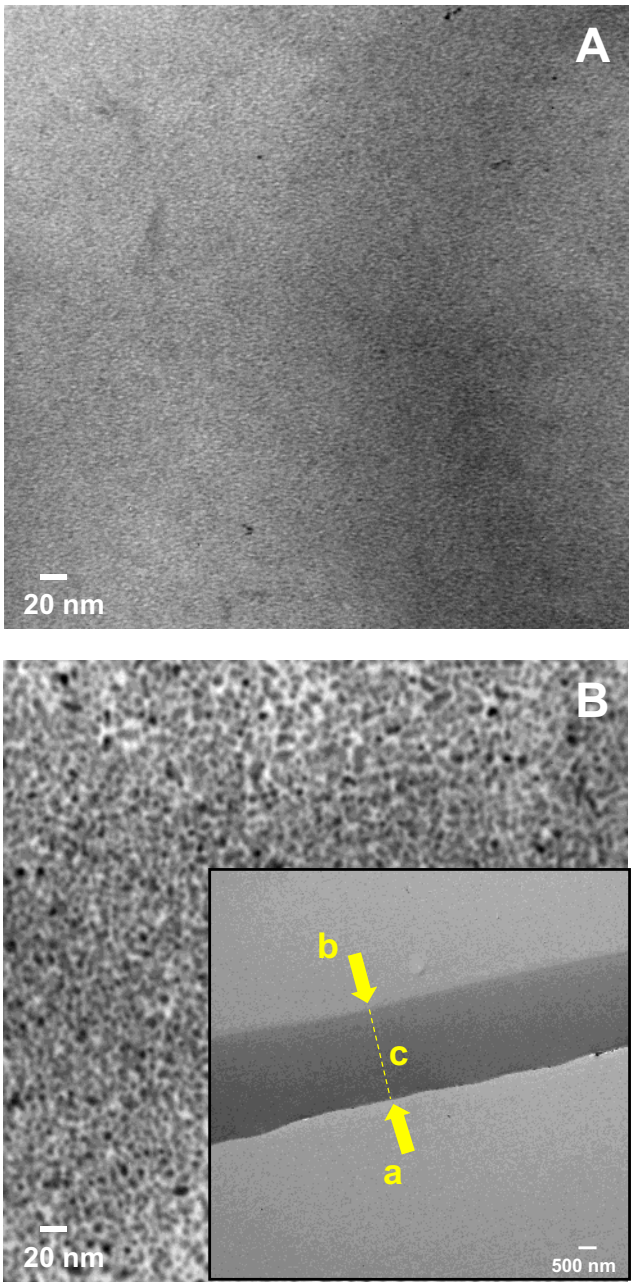

Figure 3. TEM imaging of GOx embedded MPTMS xerogel films (**A**) before and (**B**) after C6-MPC doping. Size bars in lower left corners of images are 20 nm. **Inset (B):** Cross-sectional TEM image of MPC-doped 3-MPTMS xerogel showing the pre-formed solid resin interface (a) and the outer "solution" interface (b) which define the xerogel film thickness (c). The size bar in lower right corner of inset image is 500 nm.

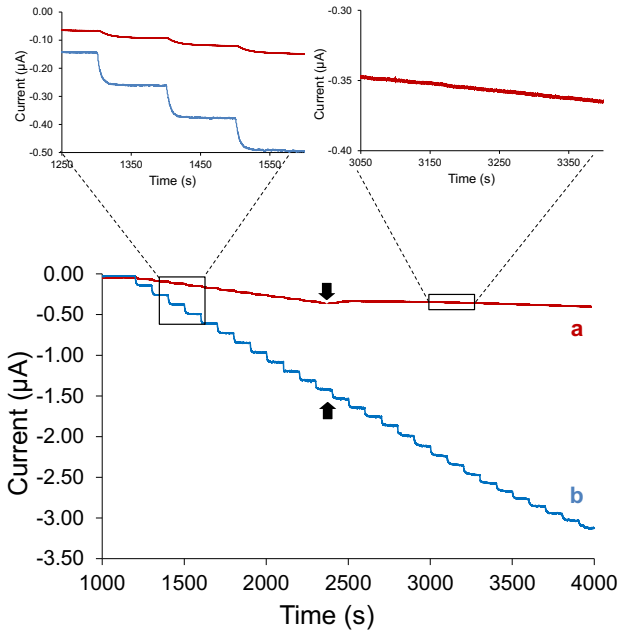

Figure 4. Representative amperometric *I-t* curves during successive 1 mM injections of glucose at platinum electrodes modified with (a) GOx embedded 3-MPTMS xerogels and (b) GOx embedded MPTMS xerogel doped with C6-MPCs, each coated with PU. MPTMS xerogels yield smaller current step responses that deteriorate (*black arrows*) whereas films incorporating the C6-MPCs produce well-defined step responses over a significantly greater range of glucose concentrations.

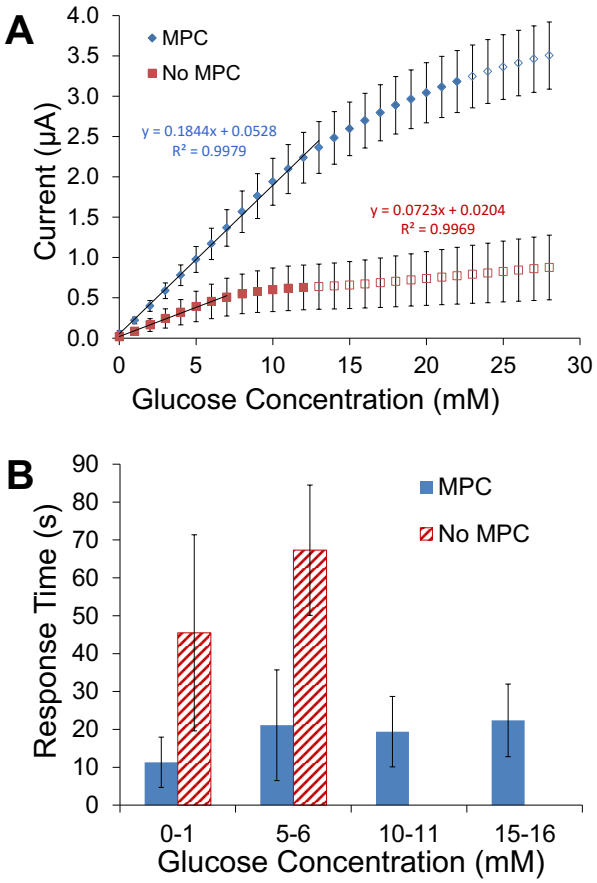

Figure 5. **(A)** Calibration curves for glucose biosensors constructed with platinum electrodes modified with GOx embedded MPTMS xerogels with and without C6-MPC doping. Solid symbols (♦,■) indicate a step-like response to glucose concentration increases whereas open symbols (◊, □) indicate a non-step response (dynamic range). **(B)** Glucose response time ($t_{r\text{-}95\%}$) comparison for increasing concentrations of glucose for sensors with and without C6-MPC doping.

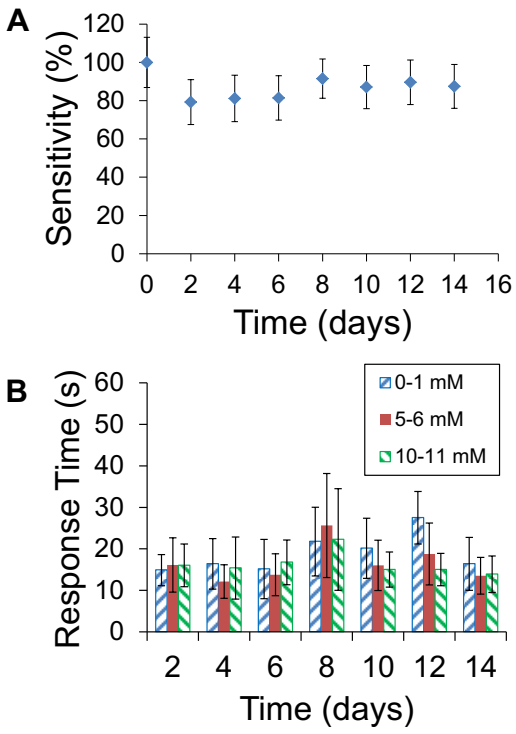

Figure 6. Stability tests of MPC-doped glucose sensors, monitored over two weeks for **(A)** percent sensitivity (derived from the slope of collected calibration curves) and **(B)** response time ($t_{r\text{-}95\%}$) at 0-1 mM, 5-6 mM, and 10-11 mM glucose injections.

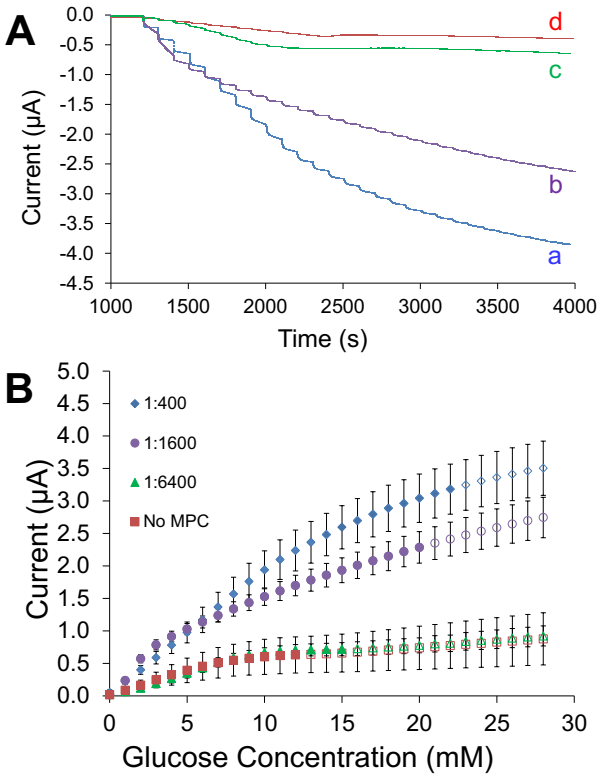

Figure 7. **(A)** Representative amperometric *I-t* curves and **(B)** corresponding calibration curves during successive injections of glucose at platinum electrodes modified with GOx embedded 3-MPTMS xerogels doped with a C6 MPC-to-silane ratio of (a) 1:400, (b) 1:1600, (c) 1:6400 or (d) no MPCs during film deposition and coated with a PU outer layer. Solid symbols (♦,●,▲,■) indicate a step-like response to glucose concentration increases whereas open symbols (◊,○, Δ, □) indicate a non-step response (dynamic range).

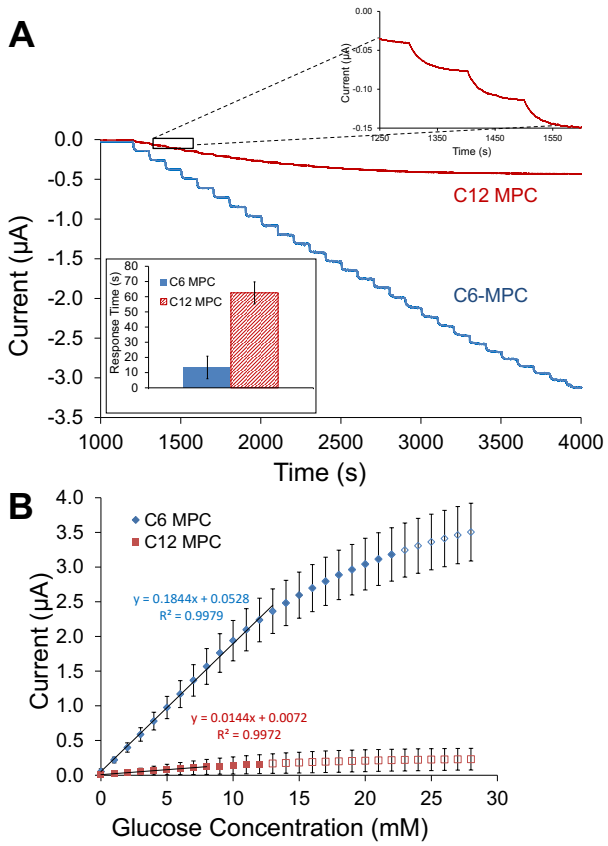

Figure 8. **(A)** Representative amperometric *I-t* curves and response times (**inset**) during successive injections of glucose at platinum electrodes modified with GOx embedded MPTMS xerogels doped with either C6-MPC or C12 (dodecanethiolate) MPC and a PU coating; **(B)** Calibration curves comparing C6-MPC versus C12 MPC doped GOx/MPTMS xerogels. Solid symbols (♦, ■) indicate a step-like response to glucose concentration increases whereas open symbols (◊, □) indicate a non-step response (dynamic range).

Graphical Abstract(3.33" x 4.76")

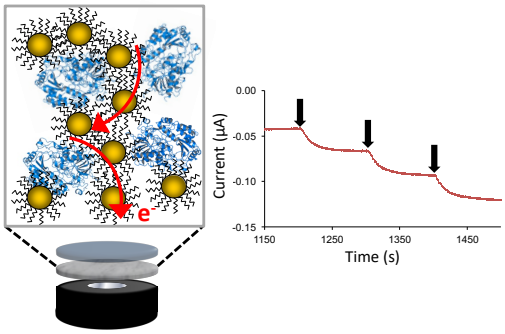
e⁻
0.00
-0.05
-0.10
-0.15
Current (µA)
1150
1250
1350
1450
Time (s)